

Introduction: imaging the brain and its diseases

R. Nick Bryan

The last several decades have seen remarkable advances in the clinical neurosciences, with some of the most remarkable achievements related to neuroimaging. Given the current depth of knowledge about the brain, it is difficult to appreciate that barely 300 years ago this organ was almost a complete mystery, particularly as to its function. While the brain has been recognized as an “organ” since antiquity, no functional role was ascribed to it until the early 1600s, when Descartes placed the “soul” in one of its small parts, the pineal gland.[1] Prior to this intriguing, but erroneous, concept, much more functional importance had been attributed to the fluid in the ventricles than to the brain itself. Descartes’ non-scientific attribution was, fortunately, quickly followed by the much more rigorous description of the structure of the brain by Thomas Willis in 1664.[2] While Willis’ application of the scientific method to the brain was seminal, the primitive scientific tools available at the time limited his direct observations to anatomy, and gross anatomy at that, which in and of itself does not convey function. Despite little direct evidence, Willis began to argue that mental functions reside in the brain, as do certain diseases such as epilepsy. The scientific tools necessary to prove his assertions by actual observation of physiology, molecular biology, and other “functional” aspects of the brain were still several centuries away.

However, the brain was found to have a peculiarly strong correlation between structure (anatomy) and function (behavior). This intimate relationship provided the basis for the still robust field of “experimental” neuroanatomy. Experimental neuroanatomy, such as the destruction of a portion of the brain in an animal followed by observations of its behavior, allowed eighteenth and early nineteenth century scientists such as Gall and Rolando to make structure–function correlations that documented the brain as a central control organ.[3,4] Since it has never been appropriate to perform debilitating experiments on humans, many fundamental questions pertaining to human brain function persisted until the “natural science” version of experimental neuroanatomy was introduced by clinicians such as Morgagni, who attributed neurological deficits such as hemiparesis to grossly destructive or functionally disruptive lesions of patients’ brains found at autopsy.[5] Broca, in 1860, applied such lesion–deficit correlation to a patient who had

suffered the acute onset of aphasia and whose brain at autopsy revealed an infarct in the right frontal operculum, thus localizing a component of speech to a particular cortical region.[6] Such “dysfunctional” imaging was subsequently employed by many clinical scientists, particularly those nineteenth and early twentieth century neurologists whose names are attached to so many neurological syndromes. While lesion–deficit correlation has been a very informative means of studying the brain, it is limited by its anatomical basis, which does not provide any direct information about the brain’s physiology or molecular makeup.

Note that all of these early methods of studying the brain involved some form of imaging. Given the spatially heterogeneous nature of the brain (both structurally and functionally), imaging of the brain is an absolute necessity in order to document the location of an experimental or natural lesion. Only with this anatomic information could the observed neurological, psychological, or cognitive dysfunction be linked to its physical source. In humans, these types of investigation were severely restricted by the unfortunate necessity of a patient having to suffer an insult to the brain and the additional burden that the patient either dies having permitted an autopsy or submits to a craniotomy. These were until very recently the only means of directly documenting the presence and extent of a brain lesion.

Despite the many drawbacks, experimental anatomy and clinical lesion–deficit research in the late 19th and early 20th century provided the basis of much of our current understanding of brain functions and their localizations. During the 20th century, these early, primitive, but informative, techniques were increasingly supplemented by more advanced histological, neurophysiological, and molecular biological techniques, which have combined to yield the great depth of knowledge about the brain that we now have, knowledge that extends from single-cell events to highly integrated cognitive functions. An early and critical technological advance involved imaging, microscopy, which revealed morphology at the cellular level. Microscopic imaging of the nervous system was pioneered by Camillo Golgi who discovered and Santiago Ramon y Cajal who applied the silver staining technique that demonstrates individual neurons.[7] Their pioneering work, which was awarded a Nobel Prize

Introduction

in 1906, laid the groundwork for the modern “neuron doctrine” and the cellular basis of many neurological diseases.[7] Histological stains steadily evolved from non-specific morphological enhancers such as the hematoxylin & eosin (H&E) stains to refined histochemical indicators such as today’s immunohistochemical techniques, which demonstrate specific proteins in their cellular milieu. Gross and microscopic morphological discoveries were accompanied and complemented by functional, neurophysiological studies, such as those of Sir Charles Sherrington, that confirmed the neuron as a discrete, functional element of the brain.

However, many of these newer techniques had, and continue to have, restrictions to their applications in humans, particularly intact, functioning humans. Histological techniques require tissue, which is never easily obtained from human brain and almost never from multiple or large regions. Many neurophysiological techniques require intrusion into the brain, such as for electrode recordings or cortical stimulation. Molecular techniques are seldom feasible in intact functioning brain. While these powerful techniques provide extraordinarily detailed information about small parts of the brain, none provide data from the entire, functioning brain. This is a significant limitation as many functions of the brain involve composite actions of its many spatially, physiologically, and biochemically disparate components. This is particularly true of complex behavioral tasks and cognition. The spatial heterogeneity of the brain has always begged for imaging of the whole organ, preferably in the intact, functioning state. This has not been feasible until very recently.

In 1974, clinical neuroscience experienced a profound change with the invention of the X-ray computed tomography (CT) scanner, an instrument that for the first time could non-invasively produce images of the whole, living human brain.[8] These CT scans are based on electron density, and there are only subtle differences of this parameter in the brain. For instance, the electron density of gray matter (GM) and white matter (WM) differ by only 0.5%. Hence, clinical CT scans yield relatively crude images of the brain. However, these relatively crude CT images allowed neuroscientists to see not only the normal human brain but also a broad spectrum of neuropathology. Brain tumors, strokes, and abscesses could be seen without the need for craniotomy or autopsy. As a result of this remarkable new machine’s ability to demonstrate the precise locations of brain lesions, the previously important practice of “surgical neurology” disappeared.

While CT scanners can only image morphology at relatively low contrast and spatial resolution, the technique allowed the traditional lesion–deficit methodology to be applied to living subjects contemporaneously with functional examinations. Autopsy and craniotomy are no longer necessary to demonstrate the anatomical correlates of functional deficits, and the literature has become replete with lesion–deficit studies that have expanded our knowledge of how the function of the human brain is spatially distributed. Investigators such as the Damasio have used clinical CT, and later magnetic resonance

(MR), scans of hundreds of neurologically, psychologically, and cognitively impaired subjects to better demonstrate the anatomic substrate of higher order mental tasks.[9] However these images still show only static anatomy and do not reflect any physiological or molecular aspect of the brain. Indeed it can be difficult to tell a conventional CT or MR scan of a cadaver’s brain from that of a living person. While we now understand many strong relationships between the gross structure and function of the brain, there remains the overpowering need to be able to directly “see” physiological and molecular functions of the brain. After all, it is more important to know what the brain is doing than what it looks like!

The need for functional and molecular imaging of the brain was initially met by the combination of positron emission tomography (PET) and metabolic radio tracers such as [¹⁸F]-fluoro-2-deoxyglucose (FDG), H₂O¹⁵, and CO¹⁵. [10] The PET methodology allows non-invasive imaging of the whole brain under resting as well as task conditions. Physiological parameters, such as cerebral blood flow (CBF), can be imaged non-invasively in the clinical environment, as can responses of these parameters to activation of the brain by a task: direct imaging of dynamic brain physiology. In addition, radio ligands have been developed that produce images of the distribution of specific molecules in the brain, such as components of neurotransmitter systems. This methodology remains a powerful research tool, albeit expensive and logistically challenging.

The development of PET imaging was followed relatively quickly by magnetic resonance imaging (MRI). This technique derived from nuclear magnetic resonance (NMR), a physical phenomenon related to the behavior of atomic nuclei in the presence of a magnetic field, which was described by Bloch, Hansen, and Packard in 1946.[11] During the 1940s and 1950s many investigators developed techniques that allowed this physical phenomenon to be exploited for the study of chemical structure. Since the introduction of the Fourier transform (FT) technique by Ernst in 1966 and the development of high-field superconducting magnets, NMR has been able to elucidate the detailed chemical structure of even large molecules such as proteins.[12] The addition of magnetic field gradients to the requisite static magnetic field of NMR can spatially define a sample, allowing MRI. This concept of the use of magnetic field gradients to generate images was first demonstrated in the landmark 1973 paper by Lauterbur [13]. In 1976, Ernst introduced the principle of two-dimensional FT NMR, which is now almost universally used for all MRI.[14]

Conventional MRI relies on radio signals emitted by nuclei of molecules, particularly H₂O, of relatively stationary tissue. Because of their different water content and relaxation times, there is typically more than a 20% difference in this signal between GM and WM. Similar differences can be found between certain pathological tissues and normal brain. This accounts for the exquisite images of normal neuroanatomy or multiple sclerosis (MS) plaques produced by contemporary MRI. The first decade of clinical MRI was characterized by steady improvements in the morphological imaging capabilities of

this quite remarkable and completely non-invasive and safe technology. However, there is little useful physiological information in the conventional MRI signal, except for that related to fast-flowing fluids such as blood. Recent MRI advances have focused on the development and application of molecular and physiological imaging capabilities. These new MRI methods are the focus of this volume and reflect the continuing evolution from purely anatomical to physiological and molecular imaging of the brain.

The three main advanced MR methods to be presented are MR spectroscopy (MRS), diffusion MR, and perfusion MR, with its near relative, functional MRI (fMRI). Magnetic resonance spectroscopy yields images of the distribution and concentration of naturally occurring molecules such as *N*-acetyl aspartate (NAA) (one of the most abundant amino acids in the brain, and believed to be localized predominantly in neurons and their processes), choline (Cho) (a key constituent of cell membranes), and lactate (Lac) (a reflection of anaerobic metabolism). Diffusion MRI demonstrates regions of normal and pathological micromolecular motion. Under appropriate conditions, these images can reflect patterns of axonal anatomy, and when applied as “fiber tracking,” this technique can turn the large, homogeneously bland regions of WM of conventional MRI into dramatic three-dimensional displays of the major axonal pathways. Using extrinsic contrast agents or intrinsic contrast agents, such as blood, perfusion MRI can create not only qualitative but also quantitative maps of various perfusion parameters, including CBF, cerebral blood volume (CBV), and vascular permeability. With slight, but important modifications, perfusion imaging techniques can, in conjunction with the performance of specific mental tasks, demonstrate local, physiological activation of the brain. Given these techniques, at last neuroscientists can painlessly, non-invasively, and safely study important physiological properties of a whole, living, functioning human brain. One can now actually see what the brain is doing, not just what it looks like.

The clinical value of these physiological and molecular tools is becoming increasingly appreciated and can be illustrated by

their applications to one disease – cerebral ischemia and stroke. Lactate is an important metabolic molecule of which little is produced by the brain under aerobic conditions. However, under anaerobic conditions, such as ischemia, abundant lactate may be produced and is easily detected by proton MRS.[15] The imaging of lactate by MRS is one of the most sensitive means of detecting even mild cerebral ischemia, its presence temporally preceding irreversible ischemia and stroke. Diffusion MRI is also very sensitive to ischemia, presumably because there is a shift of extracellular water molecules into the intracellular compartment where molecular diffusion is more restricted.[16] Even if this theory is not correct, empirically it is well established that diffusion-weighted images (DWI) show some of the earliest changes of stroke and severe ischemia. It almost goes without saying that perfusion imaging is a powerful tool for evaluating cerebral ischemia. Perfusion MRI can easily, directly, and accurately document the reduction of CBF secondary to obstructive or non-obstructive cerebral ischemia, as well as demonstrate changes in CBV that often provide additional information as to the physiological severity of the insult.[17] Such physiological tools are increasingly necessary for the management of acute cerebral ischemia when the traditional anatomical diagnosis of “live brain–dead brain” is not adequate for directing vascular or neuroprotective treatment.

The authors of the chapters of this book describe the latest physiological and molecular MRI methodologies in detail and then illustrate their applications to major diseases of the brain, including cerebrovascular and degenerative diseases, neoplasia, seizure, inflammation, trauma, and even psychiatric disorders. These new techniques of the early twenty-first century foreshadow even more remarkable advances in neuroimaging, but first, please, appreciate the robust functional imaging capabilities so well described and illustrated in this volume. This revised edition includes updated material reflecting the increased maturity and clinical use of MRS, diffusion tensor imaging (DTI), and perfusion studies. New sections on the use of fMRI for presurgical planning as well as susceptibility and contrast-based permeability imaging are also provided.

References

- Descartes R. Rules for the direction of the mind. Discourse on the method. Meditations on first philosophy. Objections against the meditations and replies. The Geometry. In *Great Books of the Western World*. Vol. 31. ed. in chief Hutchins JA. Chicago, IL: Encyclopedia Britannica, 1952.
- Willis T. *Cerebri Anatome*, 1664. [Trans. Pordage S. Birmingham, AL: Classics of Medicine Library.]
- Gall FJ. *Gall's Works. On the Functions of the Brain and Each of Its Parts*, 1835. [trans Lewis W. Boston, MA: Marsh, Capen & Lyon.]
- Marshall LH, Magoun HW. *Discoveries in the Human Brain*. Totowa, NJ: Humana Press, 1998.
- Morgagni JB. *The Seats and Causes of Diseases*, 1760. [Trans. Alexander B. Birmingham, AL: Classics of Medicine Library.]
- Broca P. Remarques sur le siège de la faculté du langage articulé, suivies d'une observation d'aphémie. *Bull Soc Anat Paris* 1861; 330–357. [Trans. von Boninn G. *Some Papers on the Cerebral Cortex*. Springfield, IL: C.C. Thomas, 1960.]
- Henry, J. Neurons and Nobel Prizes: A centennial history of neuropathology. *Neurosurgery* 1998; 42: 143–156.
- Hounsfield GN. Computerized transverse axial scanning (tomography): part 1. Description of system. *Br J Radiol* 1973; 46: 1016–1022.
- Damasio H, Damasio AR. *Lesion Analysis in Neuropsychology*. New York: Oxford University Press, 1989.
- Fox PF, Raichle ME, et al. Nonoxidative glucose consumption during focal physiologic neural activity. *Science* 1988; 241: 462–464.
- Bloch F, Hansen WW, Packard M. The nuclear induction experiment. *Phys Rev* 1946; 70: 474–485.
- Ernst RR, Anderson WA. *Rev Sci Instrum* 1966; 37: 93.

Introduction

13. Lauterbur PC. Image formation by induced local interactions: examples employing nuclear magnetic resonance. *Nature* 1973; **242**: 190–191.
14. Aue WP, Bartholdi E, Ernst RR. Two-dimensional spectroscopy. Application to nuclear magnetic resonance. *J Chem Phys* 1976; **64**: 2229.
15. Barker PB, Gillard JH, van Zijl PCM, *et al.* Acute stroke: evaluation with serial proton magnetic resonance spectroscopy. *Radiology* 1994; **192**: 723–732.
16. Le Bihan D, Breton E, Lallemand D. MR imaging of intravoxel incoherent motions: application to diffusion and perfusion in neurologic disorders. *Radiology* 1986; **161**: 401–407.
17. Rempp KA, Brix G, Wenz F, *et al.* Quantification of regional cerebral blood flow and volume with dynamic susceptibility contrast-enhanced MR imaging. *Radiology* 1994; **193**: 637–641.

Section 1
Chapter

Physiological MR techniques

Fundamentals of MR spectroscopy

Peter B. Barker

Introduction

Nuclear magnetic resonance (NMR) spectroscopy was demonstrated for the first time in bulk matter in 1945 when Bloch and Purcell independently demonstrated that a strong magnetic field induced splitting of the nuclear spin energy levels, resulting in a detectable resonance phenomenon.[1,2] The method was originally of interest only to physicists for the measurement of the so-called gyromagnetic ratios (γ) of different nuclei, but applications of NMR to chemistry became apparent after the discovery of chemical shift and spin-spin coupling effects in 1950 and 1951 respectively.[3,4] High-resolution liquid state NMR spectra contain fine structure because the resonance frequency of each molecule is influenced by both neighboring nuclei (coupling) and the chemical environment (shift), which allows information on the structure of the molecule to be deduced. Hence, NMR spectroscopy rapidly became an important, and widely used, technique for chemical analysis and structure elucidation of chemical and biological molecules.

Major technical advances in the 1960s included the introduction of superconducting magnets (1965), which were very stable and allowed higher field strengths to be attained than with conventional electromagnets, and in 1966 the use of the Fourier transform (FT) for signal processing. In FT spectroscopy, the sample is subjected to periodic radiofrequency transmitter pulses followed by collection of the signal as a function of time (i.e., a time-domain signal), and the frequency-domain spectrum is calculated by FT. Use of FT NMR provides increased sensitivity compared with previous (so-called “continuous-wave”) techniques, and also led to the development of a huge variety of pulsed NMR methods, including multidimensional NMR techniques.

Biological and medical applications of magnetic resonance were developed in the early 1970s with the introduction of magnetic resonance imaging (MRI) and magnetic resonance spectroscopy (MRS) of biological tissue. In vivo MRS of humans became possible in the early 1980s with the advent of whole-body magnets with sufficiently high field strength and homogeneity.[5] Early studies focused on the phosphorus nucleus, since this was the most technically feasible at that time. Methods were developed for spatially localized ^{31}P MRS,[6] and studies of major neuropathology (such as

stroke or brain tumors) were performed.[7,8] A significant problem with ^{31}P MRS, however, is its low sensitivity (mainly because of the relatively low gyromagnetic ratio of ^{31}P , and low concentrations of phosphorus-containing compounds). Since spatial resolution in in vivo spectroscopy is largely limited by the available signal-to-noise ratio (SNR), the minimum voxel size for ^{31}P spectroscopy of the human brain is typically 30 cm^3 using conventional techniques and 1.5 tesla (1.5 T) magnets. This resolution is generally too coarse for many clinical applications involving focal brain lesions.

In recent years, there has been more interest in proton MRS, particularly after it was demonstrated that it was possible to obtain high-resolution spectra from small, well-defined regions in reasonably short scan times.[9] The higher sensitivity of the proton results from several factors, including higher gyromagnetic ratio, higher metabolite concentrations, and more favorable relaxation times. Although proton spectroscopy has been demonstrated in a number of organ systems (in particular, recent studies show promise for the use of proton spectroscopy in the diagnosis of prostate and breast cancer), the overwhelming number of applications have been in the brain, because of the absence of free lipid signals in normal cerebrum, relative ease of shimming, and lack of motion artifacts. The proton is also a widely used nucleus because it is the same nucleus used for conventional MRI, and therefore it is usually possible to perform proton MRS on most clinical MRI machines without the need to purchase additional scanner hardware or modifications, provided that suitable software is available.

In fact, NMR spectroscopy can be performed with many different nuclei, and in the brain, in addition to ^1H and ^{31}P , there have been reports of spectroscopy of deuterium (^2D), ^{13}C , ^{15}N , ^7Li , ^{23}Na , and ^{19}F , using either signals from endogenous nuclei and/or compounds, or using signals from administration of (sometimes isotopically enriched) exogenous substances. All of these studies fall into the context of advanced research at the current time and, therefore, will not be considered further here. This chapter focuses on the information content of proton MR spectra of the brain, technical issues such as choice of localization technique, and normal age-related and anatomical variations.

Section 1: Physiological MR techniques

Information content of proton MR spectra of the brain

Figure 1.1 shows examples of proton spectra recorded at long and short echo times (TE). The assignment and significance of each the resonances in the spectrum is discussed below and summarized in Table 1.1.

N-Acetyl aspartate

The largest metabolite signal, resonating at 2.02 parts per million (ppm), occurs from the *N*-acetyl group of *N*-acetyl aspartate (NAA), with a smaller contribution from *N*-acetylaspartyl glutamate (NAAG), particularly in white matter.[10] Despite being one of the most abundant amino acids in the central nervous system (CNS), NAA was not discovered in the brain until 1956 and its function has been the subject of considerable debate. It has been speculated to be a source of acetyl groups for lipid synthesis, a regulator of protein synthesis, a storage form of acetyl-CoA or aspartate, a breakdown product of NAAG, a “molecular water pump,” or an osmolyte.[11] Using immunocytochemical techniques, NAA has been shown to be predominantly localized to neurons, axons, and dendrites within the CNS,[12] and studies of diseases known to involve neuronal

and/or axonal loss (infarcts, brain tumors, seizure foci, multiple sclerosis [MS] plaques, for example) have uniformly shown NAA to be decreased. In pathologies such as MS, correlations between brain levels and clinical measures of disability have been shown.[13] Animal models of chronic neuronal injury have also been shown to give good correlations between NAA levels (as measured by MRS) and *in vitro* measures of neuronal survival.[12,14]

For all these reasons, it has been tempting to “label” NAA as a neuronal marker, and to equate levels of NAA with neuronal density. However, there is also evidence that this may not always be the case. For instance, NAA has been detected in non-neuronal cell types *in vitro*, such as mast cells or isolated oligodendrocyte preparations, suggesting that NAA may not be specific for neuronal processes,[15–17] although it is not completely clear if these cells are present in the brain at high concentrations, or if their metabolism is identical, *in vivo*. It is also well known that there are exceptions to the correlation between neuronal density and NAA levels. For instance, the pediatric leukoencephalopathy Canavan’s disease is associated with a large elevation of intracellular NAA owing to deficiency of aspartoacylase, the enzyme that degrades NAA to acetate and aspartate (Fig. 1.2).[18] In addition, there has been a case report of a young boy with mental retardation with an

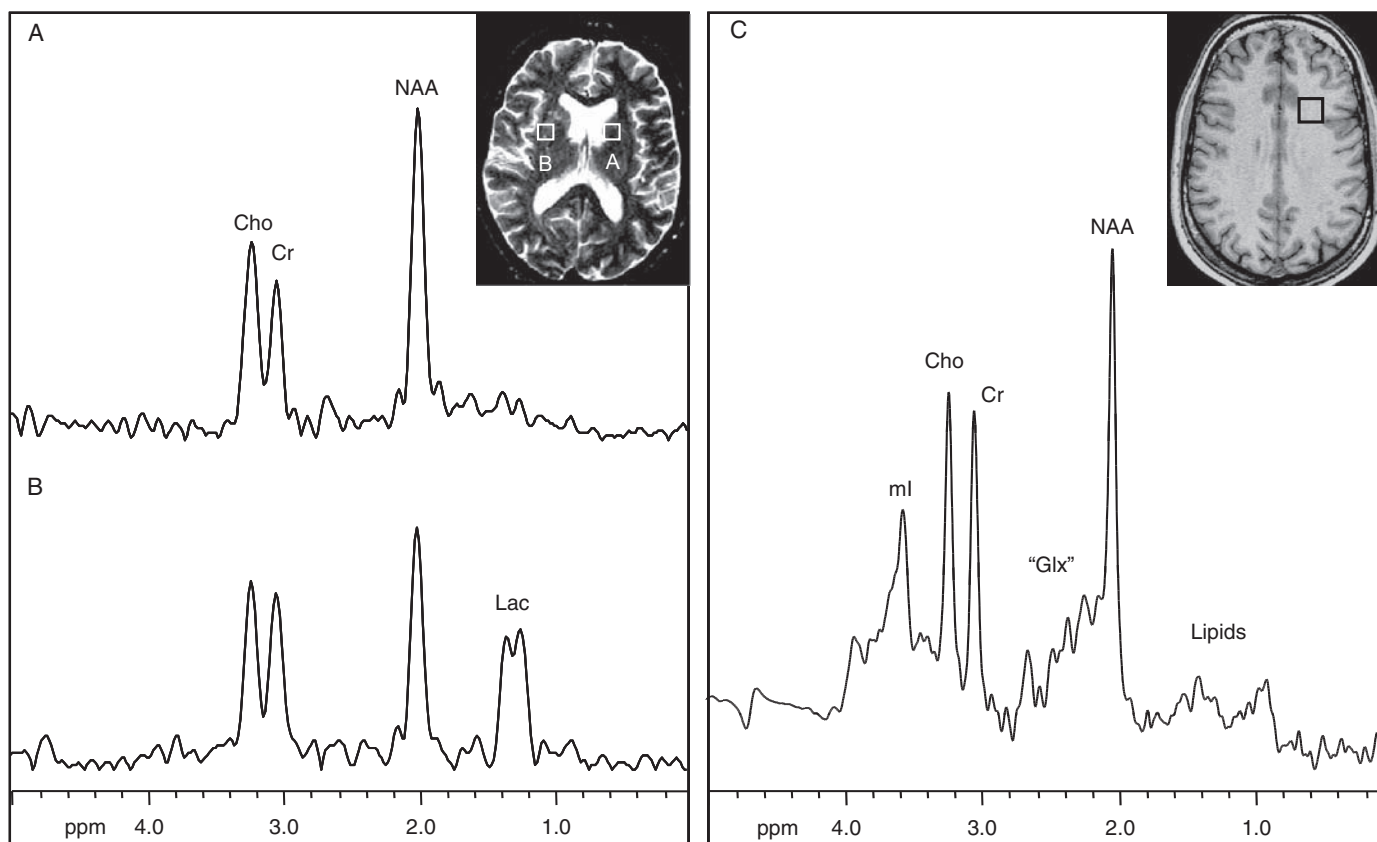


Fig. 1.1 Proton spectra of the human brain recorded at both long (272 ms) (A,B) and short (35 ms) (C) echo times (TE). In the long TE spectra from a patient with an acute right middle cerebral artery stroke, the normal spectrum (A) from the left hemisphere shows signals from choline (Cho), creatine (Cr) and *N*-acetyl aspartate (NAA). In the ischemic left hemisphere (B) an additional signal from lactate (Lac) is apparent as well as a moderate decrease in NAA. In the short TE spectrum of normal frontal white matter (C), in addition to NAA, Cr and Cho, signals can be detected from *myo*-inositol (ml), glutamine and glutamate (Glx), and lipids. (A) and (B) are from a multislice MRSI data set (nominal voxel size 0.8 cm³), while (C) is recorded from an 8 cm³ single voxel using the PRESS sequence.

Table 1.1 Metabolites detected in the brain by proton MR spectroscopy

Compounds normally present	Compounds which may be detected under pathological or other abnormal conditions
<i>Large signals at long TE</i>	<i>Long TE</i>
N-Acetyl aspartate (NAA)	Lactate (Lac)
Creatine (Cr) and phosphocreatine (PCr)	β -Hydroxybutyrate, acetone
Choline compounds (Cho): glycerophosphocholine (GPC), phosphocholine (PC), free choline (Cho)	Succinate, pyruvate
	Alanine
	Glycine
<i>Large signals at short TE</i>	<i>Short TE</i>
Glutamate (Glu)	Lipids
Glutamine (Gln)	Macromolecules
<i>myo</i> -Inositol (ml)	Phenylalanine
	Galactitol
<i>Small signals (short or long TE)</i>	<i>Exogenous compounds (short or long TE)</i>
N-Acetylaspartyl glutamate (NAAG), aspartate	Propan-1,2-diol
Taurine, betaine, <i>scyllo</i> -inositol, ethanolamine	Mannitol
	Ethanol
Glucose, glycogen	Methylsulfonylmethane (MSM)
Purine nucleotides	
Histidine	
<i>Small signals that can be detected with the use of 2D and/or spectral editing techniques</i>	
γ -Aminobutyric acid (GABA)	
Homocarnosine, pyrrolidinone	
Glutathione	
Threonine	
Vitamin C (ascorbic acid)	

apparently global complete absence of NAA (Fig. 1.2).[19] Clearly, in these subjects, the high or absent levels of NAA do not reflect changes in neuronal density but rather a perturbation of the synthetic and degradation pathways of NAA metabolism (Fig. 1.2). Further examples of the lack of direct correlation of NAA and neuronal density are various pathologies that have shown either spontaneous or treatment-related reversal of decreased NAA. Some examples include MS, mitochondrial diseases, the acquired immunodeficiency disease (AIDS), temporal lobe epilepsy, amyotrophic lateral sclerosis, and acute disseminated encephalomyelitis.[11,20] (Fig. 1.3). Since it is not clear that these cases involve increased numbers of neurons over time, it is more likely that the increases in NAA result from alterations in NAA metabolism as a response to treatment (or spontaneous recovery).

It should be remembered that the macroscopic concentration of NAA (like that of any neurochemical) depends on the

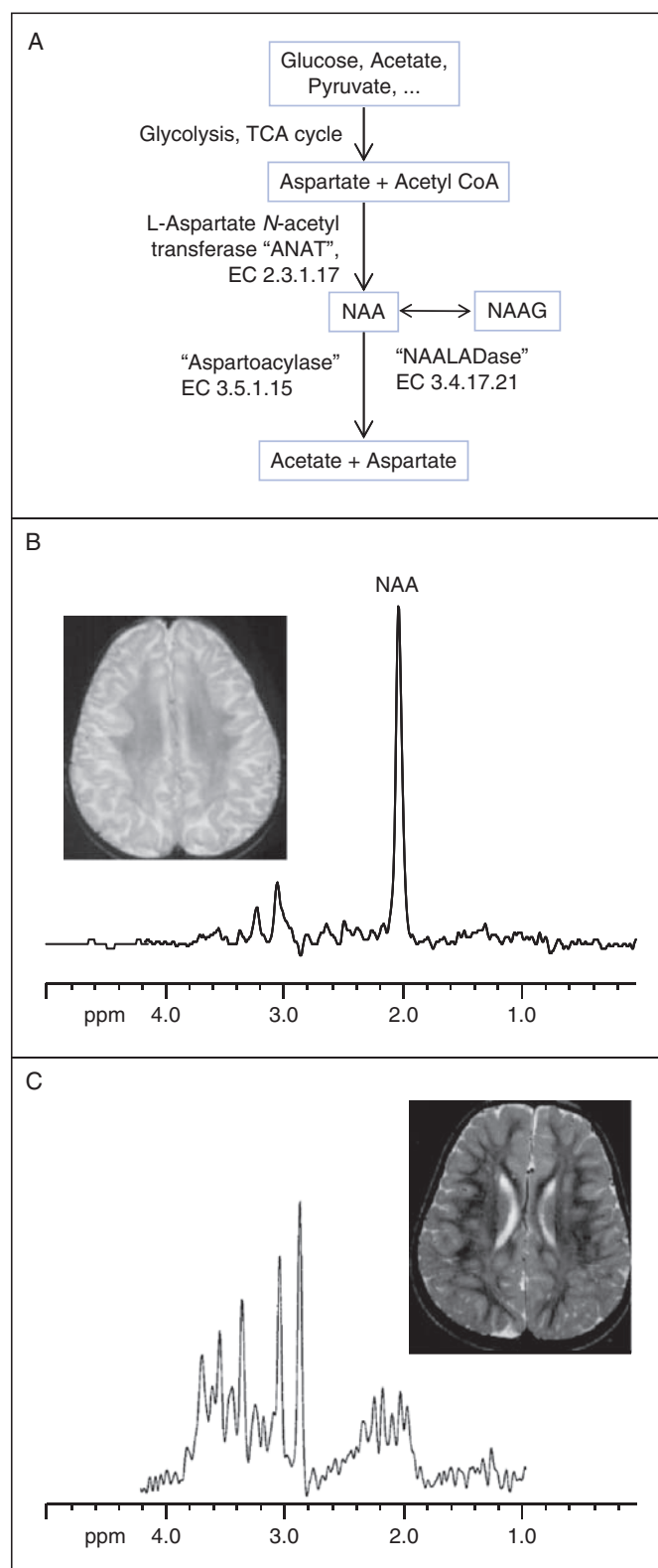


Fig. 1.2 Some biochemical pathways involving *N*-acetyl aspartate (NAA) (A) and pathological processes involving NAA metabolism (B,C). (B) Long echo time (270 ms) proton spectra of the frontal white matter in a child with Canavan's disease, showing a high ratio of NAA/creatine (Cr) (and NAA to other metabolites) owing to the lack of the enzyme aspartoacylase, which degrades NAA. The T_2 -weighted MRI shows a near complete lack of myelination. (C) A 3-year-old boy with mental retardation and complete absence of NAA on brain MRS (short echo time). The MRI is only mildly abnormal, while other metabolites in the spectrum are also in the normal range. A deficit in the NAA synthetic pathway was suspected, but not proven. (Reproduced with permission from Martin *et al.* [19]).

Section 1: Physiological MR techniques

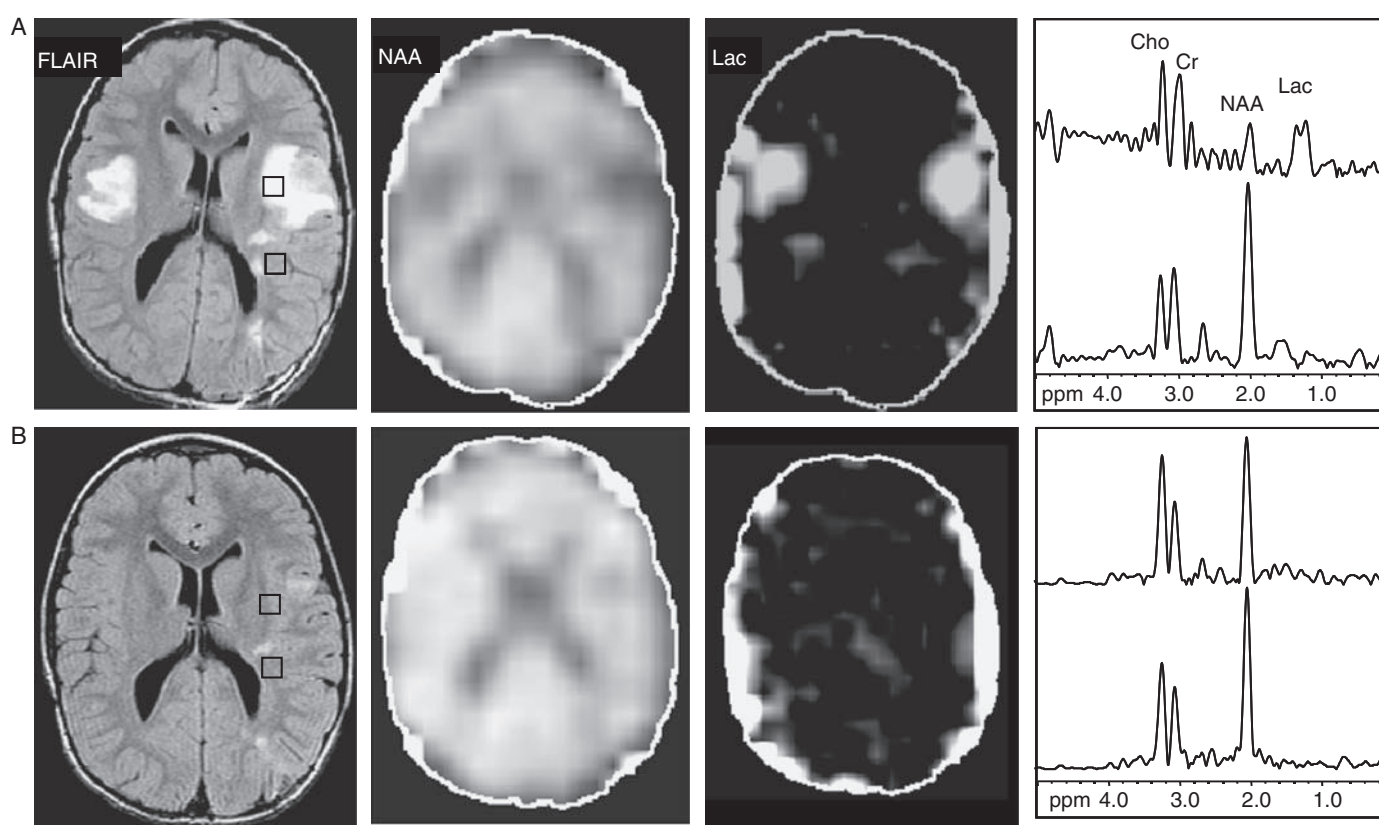


Fig. 1.3 An example of a reversible reduction in *N*-acetyl aspartate (NAA) in a 6-year-old child with acute disseminated encephalomyelitis. (A) At 36 days after symptom onset, FLAIR MRI shows multiple, bilateral lesions that are characterized by reduced levels of NAA and increased lactate on MRS. Choline (Cho) and creatine (Cr) are within the normal range. (B) At day 137 after steroid treatment, the lesions have nearly resolved, and the spectra are more normal, in particular NAA has partially recovered and lactate is now undetectable.

fluxes of synthetic and degradation pathways, as well as cellular density and brain water content and distribution. Sometimes, a decrease in NAA may be solely or largely attributable simply to increased extracellular water or cerebrospinal fluid (CSF) content within the localized MRS volume, although these factors can be corrected with appropriate analysis techniques (Ch. 2). Neuronal and axonal dysfunction or loss should be considered when the tissue NAA content is reduced, because the balance of evidence suggests that the majority of NAA is located within neuronal processes. Whether the reduction represents an irreversible loss of cells or a potentially reversible metabolic process will in large part depend on the individual pathology in which it is encountered, and the prognosis for recovery of brain function is presumably also variable. In certain types of lesion (e.g., chronic infarction, brain tumors), it appears likely that reduction in NAA does indeed correspond to irreversible neuronal loss. Overall, non-invasive MRS measurements of NAA appear to be one of the best *surrogate* markers currently available for neuronal integrity in many neurological and psychiatric disorders.

Choline

The “choline” signal (“Cho,” 3.24 ppm) arises from the $-N(CH_3)_3$ groups of glycerophosphocholine (GPC), phosphocholine (PC),

and a small amount of free choline, compounds which are involved in membrane synthesis and degradation. Both increases and decreases in Cho have been reported in pathological conditions: processes leading to elevation of the Cho signal include active demyelination,[21] resulting from the degradation of myelin phospholipids, primarily to GPC, or increased numbers of glial cells.[22,23] Low Cho has been observed in hepatic encephalopathy,[24] and there is also some evidence to suggest that dietary intake of choline can modulate cerebral Cho levels.[25] Elevated Cho seems to be a characteristic of many types of neoplasm, including high-grade brain tumors (provided that they are not necrotic), prostate, breast, head and neck, and others.

Creatine

The “creatine” signal (“Cr,” 3.02 ppm) is a composite peak consisting of creatine and phosphocreatine, compounds which are involved in energy metabolism via the creatine kinase reaction generating adenosine triphosphate (ATP). Since creatine is synthesized in liver, chronic liver disease leads to lower cerebral creatine concentration.[26] There is also a rare group of diseases which involve total Cr deficiency in the brain, creatine resulting from either lack of synthesis in the liver (guanidinoacetate methyltransferase deficiency) or defective transport to the brain.[27–29] In vitro, glial cells contain a two- to four-fold

higher concentration of creatine than do neurons,[30] although curiously white matter Cr levels are lower than those of gray matter in the normal brain.

It has been suggested that the sum of creatine and phosphocreatine is relatively constant in the human brain; for this reason Cr is often used as a reference signal, and it is a common practice for metabolite ratios to be expressed as a ratio relative to Cr. However, with the development of quantitative analysis techniques, it is clear that total Cr is not constant, either in different brain regions or in pathological processes, so the assumption of Cr as an invariable reference signal should be made with caution. Absolute metabolite quantification techniques are discussed in detail in Ch. 2.

Lactate

In normal human brain, lactate (Lac; 1.33 ppm) is usually below the limit of detectability in most *in vivo* MRS studies. Any detectable brain lactate signal can, therefore, be considered abnormal, although occasionally lactate may be detectable in the CSF of normal subjects (particularly under high SNR conditions in subjects with prominent ventricles). Increased lactate is usually the result of deranged energy metabolism and has been observed in ischemia (both acute [highest] and chronic [31,32]) brain tumors,[33] mitochondrial diseases,[34] and other conditions. Small elevations of lactate have also been reported in the visual cortex during photic stimulation,[35] believed to be the result of increased non-oxidative glycolysis, but this effect does not appear to be particularly reproducible.[36] More recently, detailed investigations in humans at very high field (7 T) have suggested that lactate increases with visual stimulation do occur but are very small in amplitude (0.2 $\mu\text{mol/l}$ per g tissue, compared with its resting state concentration of approximately 1 $\mu\text{mol/l}$ per g) and, therefore, very hard to detect reliably in individual subjects.[37,38]

myo-Inositol

At short TE, additional compounds are detected that are not visible at long TE, either because of short T_2 relaxation times and/or the dephasing effects of J-coupling (Fig. 1.1C). One of the largest signals occurs from *myo*-inositol (mI) at 3.56 ppm. *myo*-Inositol is a pentose sugar, which is part of the inositol triphosphate intracellular second messenger system. Levels have been found to be reduced in hepatic encephalopathy,[26] and increased in Alzheimer's dementia,[39] low-grade brain tumors,[40] and demyelinating diseases.[41] The exact pathophysiological significance of alterations in mI is uncertain, although a leading hypothesis is that elevated mI reflects increased populations of glial cells, which are known to express higher levels of this metabolite than neurons;[42,43] this may be related to differences in the mI/Na⁺ cotransporter activity, which appears to play a key role in astrocyte osmoregulation.[44] The role of mI as an osmolyte may explain both chronic (e.g., in degenerative and inflammatory disease) and transient disturbance in mI in hypo- and hyperosmolar states (e.g., hyper- or hyponatremia).[45,46]

Glutamate and glutamine

Glutamate (Glu) and glutamine (Gln) are difficult to separate in proton spectra at 1.5 T (and are often labeled as a composite peak "Glx"), although some authors have attempted to distinguish them.[24] At very high fields (at 4 T or above), the C4 resonances of Glu and Gln start to resolve, and the detection of each separately can be reliably performed with appropriate data collection and analysis techniques (e.g., at 7 T).[47] Increased cerebral Gln has been found in patients with liver failure (hepatic encephalopathy,[26] Reye's syndrome [48]) as the result of increased blood ammonia levels, which increases Gln synthesis.

Glutamate is the most abundant amino acid in the brain and is the dominant neurotransmitter.[49] During neuronal excitation, Glu is released and diffuses across the synapse, where it is rapidly taken up by astrocytes (along with Na⁺). The astrocyte converts the Glu to Gln, which is then released and taken up again by neurons. In the neuron, Gln is converted back to Glu, and the process repeated. This Glu-Gln cycling is an energy-demanding process, which has been speculated to consume as much as 80 to 90% of the total cortical glucose usage.[50]

Less commonly detected compounds

A survey of the literature reveals some 25 additional compounds that have been assigned in proton spectra of the human brain. Some of these compounds are present in normal circumstances, but because they are very small and/or have overlapping peaks it is usually difficult to detect them. Some examples of these include NAAG, aspartate, taurine, *scyllo*-inositol, betaine, ethanolamine, purine nucleotides, histidine, glucose, and glycogen.[51] Other compounds are yet more difficult to detect and require the use of special spectral editing pulses to detect (beyond the scope of the current chapter); examples of these include γ -aminobutyric acid (GABA), glutathione, and certain macromolecules.[52,53]

Under disease conditions, other compounds may become detectable because their concentration is pathologically increased. Examples of compounds that have been detected under pathological conditions include the ketone bodies β -hydroxybutyrate and acetone,[54,55] and other compounds such as phenylalanine (in phenylketonuria),[56] galactitol, ribitol, and arabitol (in "polyol disease"),[57] succinate, pyruvate, alanine, glycine, and threonine. Finally, exogenous compounds that are able to cross the blood-brain barrier (BBB) may also reach sufficiently high concentrations to be detected by proton MRS. Examples of exogenous compounds, sometimes termed "xenobiotics," include the drug delivery vehicle propan-1,2-diol,[58] mannitol (used to reduce swelling and edema in neurosurgical procedures and intensive care), ethanol,[59] and the health food supplement methylsulfonylmethane (MSM).[60]

In order for a compound to be detectable by proton MRS *in vivo*, a rule of thumb is that its concentration should be 1 mmol/L (or 1 $\mu\text{mol/g}$ tissue) or greater, and it should be a small, mobile molecule. Hence large and/or membrane-associated molecules will not be detected. Mobile lipid moieties

Section 1: Physiological MR techniques

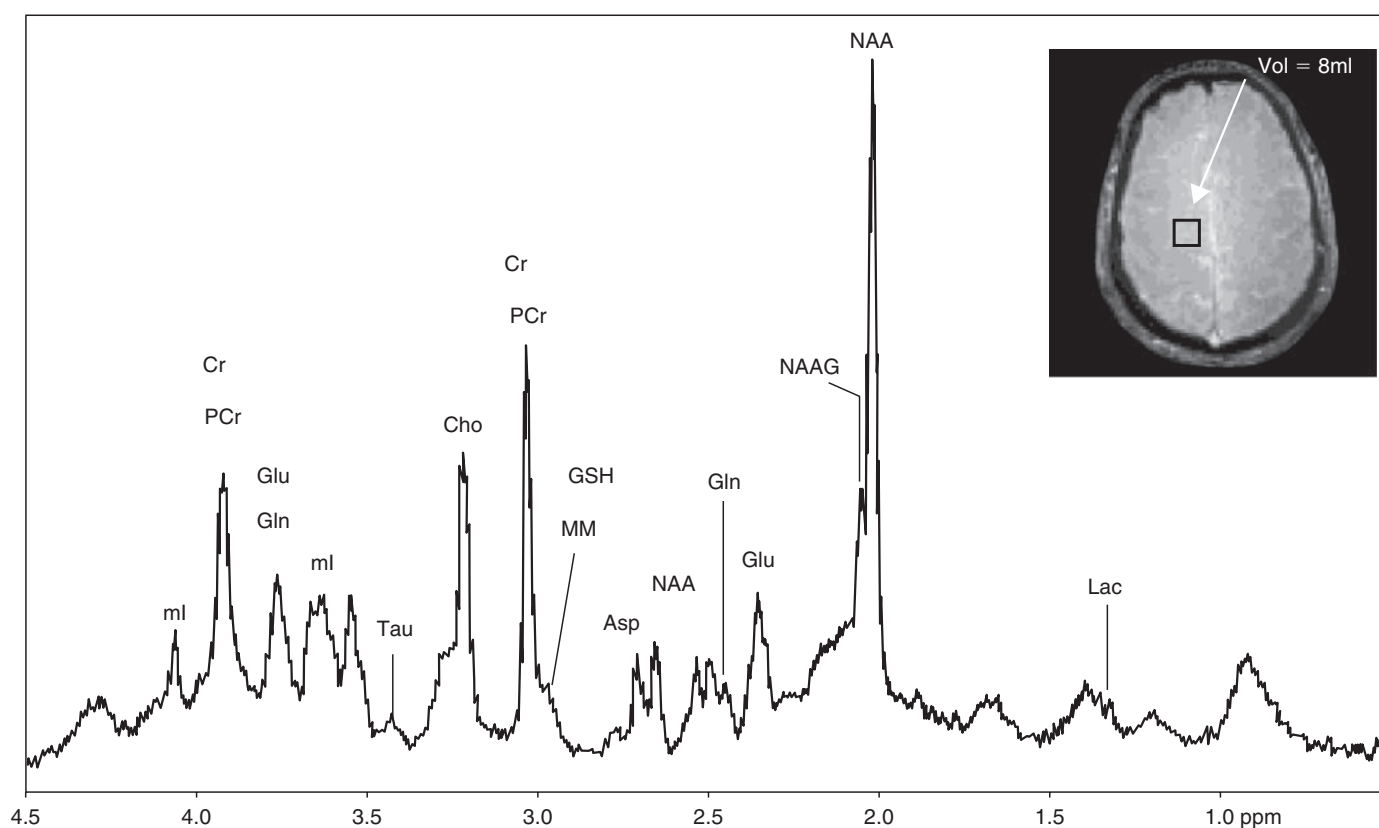


Fig. 1.4 Proton MR spectrum from parietal white matter measured at 7 T in the normal human brain STEAM; TE, 5.6 ms; TM, 5, 32 ms; TR, 5 s; voxel size, 5.8 ml; 160 averages; scan time \sim 13 min; resolution enhancement by a shifted Gaussian function. Inset shows gradient echo transverse MRI with the voxel location. (Reproduced with permission from Tkac *et al.*[47]).

from cellular membrane components are not usually detectable in normal brain at 1.5 and 3 T. Broad methyl ($-\text{CH}_3$, 0.9 ppm) and methylene ($-\text{CH}_2$, 1.3 ppm) lipid resonances may be associated with pathological necrosis, for example in the context of aggressive neoplasms (Ch. 23) or acute demyelination (Ch. 31). Because of their short T_2 , these are most commonly detected at short TE (e.g. 30–35 ms), where the methylene resonance overlaps with the 1.35 ppm lactate doublet. It has been widely assumed that they arise from disrupted membrane phospholipid bilayer, but there is also evidence that intra- or extracellular microscopic lipid droplets may contribute to the signal.

The ability to detect and quantify compounds should increase with increasing magnetic field strength; for instance, a recent study of the normal human brain at 7 T was able to detect more than 14 different compounds (Fig. 1.4).

Recently, measurements of brain temperature have also been made using the water–NAA chemical shift difference (the water chemical shift has a 0.01 ppm/ $^{\circ}\text{C}$ temperature dependence).[61]

Technical issues: spatial localization

Single-voxel techniques

Generally, two different approaches are used for proton spectroscopy of the brain: single-voxel methods based on the stimulated echo acquisition mode (STEAM) [9] or point resolved spectroscopy (PRESS) [62] pulse sequences, or MR spectroscopic

imaging (SI: MRSI, also known as chemical shift imaging [CSI]) studies usually done in two dimensions (2D) using a variety of different pulse sequences (spin echo, PRESS).[63–65].

The basic principle underlying single-voxel localization techniques is to use three mutually orthogonal slice-selective pulses and design the pulse sequence to collect only the echo signal from the point (voxel) in space where all three slices intersect (Fig. 1.5). The two most commonly used sequences are STEAM and PRESS. In STEAM (Fig. 1.5B), three 90° pulses are used, and the “stimulated echo” is collected. All other signals (“spin echoes”) are dephased by the large crusher gradient applied during the so-called mixing time (TM). Crusher gradients applied during TE on selected gradient channels are also necessary for consistent formation of the stimulated echo and removal of unwanted coherences. In PRESS, the second and third pulses are refocusing (180°) pulses, and crusher gradients are applied around these pulses to select the desired spin echo signal, and dephase unwanted coherences. There has been a detailed comparison of STEAM and PRESS;[66] they are generally similar but differ in a few key respects.

Slice profile (i.e., sharpness of edges of voxel). STEAM is somewhat better because it is easier to produce a 90° pulse with a sharp slice profile than a 180° .

Signal-to-noise ratio. Provided that equal volumes of tissue are observed and using the same parameters (repetition time